

3/17
3/12/81
11-12-81
J. R. (a)

①

38264

DR 65

UCRL-52985 Rev. 1

MASTER

Mechanical and thermomechanical calculations related to the storage of spent nuclear-fuel assemblies in granite

T. R. Butkovich

August 1981



Mechanical and thermomechanical calculations related to the storage of spent nuclear-fuel assemblies in granite

T. R. Butkovich

Manuscript date: May 1980

DISCLAIMER

LAWRENCE LIVERMORE LABORATORY
University of California • Livermore, California • 94550 

Available from: National Technical Information Service • U.S. Department of Commerce
5285 Port Royal Road • Springfield, VA 22161 • \$5.00 per copy • (Microfiche \$3.50)

CONTENTS

Foreword	ii
Abstract	1
Introduction	1
Layout of the Test Repository and Acquisition of Data	2
Calculational Input	2
Thermal Calculations	6
Thermomechanical Calculations and Results	8
Summary and Remarks	9
Acknowledgment	9
References	15

Mechanical and thermomechanical calculations related to the storage of spent nuclear-fuel assemblies in granite

ABSTRACT

A generic test of the geologic storage of spent-fuel assemblies from an operating nuclear reactor is being made by the Lawrence Livermore National Laboratory at the U.S. Department of Energy's Nevada Test Site. The spent-fuel assemblies were emplaced at a depth of 420 m (1370 ft) below the surface in a typical granite and will be retrieved at a later time. The early time, close-in thermal history of this type of repository is being simulated with spent-fuel and electrically heated canisters in a central drift, with auxiliary heaters in two parallel side drifts. Prior to emplacement of the spent-fuel canisters, preliminary calculations were made using a pair of existing finite-element codes.

Calculational modeling of a spent-fuel repository requires a code with a multiple capability. The effects of both the mining operation and the thermal load on the existing stress fields and the resultant displacements of the rock around the repository must be calculated. The thermal loading for each point in the rock is affected by heat transfer through conduction, radiation, and normal convection, as well as by ventilation of the drifts. Both the ADINA stress code and the compatible ADINAT heat-flow code were used to perform the calculations because they satisfied the requirements of this project. ADINAT was adapted to calculate radiative and convective heat transfer across the drifts and to model the effects of ventilation in the drifts, while the existing isotropic elastic model was used with the ADINA code.

The results of the calculation are intended to provide a base with which to compare temperature, stress, and displacement data taken during the planned 5-yr duration of the test. In this way, it will be possible to determine how the existing jointing in the rock influences the results as compared with a homogeneous, isotropic rock mass. Later, new models will be introduced into ADINA to account for the effects of jointing.

INTRODUCTION

The Lawrence Livermore National Laboratory (LLNL) is conducting a generic test of the geologic storage of spent-fuel assemblies from an operating nuclear reactor by emplacing these assemblies in Climax Stock granite at the U.S. Department of Energy's Nevada Test Site. The primary objectives of this test are to evaluate granite as a medium for deep geologic disposal of high-level reactor waste and to provide data on the thermal and thermomechanical behaviors of the granite surrounding this nuclear-waste repository. With these data, we expect to develop a computational technique that will model the actual behavior of the test repository. If we can model the effects of thermal loading to a few percent in tens of meters for a few years, we can have confidence that, with the same model, we can predict the behavior in the same medium for much greater distances over hundreds of years. The type of problem we are attacking lies in the realm of heat transfer and rock mechanics.

There are excellent heat-transfer codes available within the scientific community, but, for rock mechanics, the available computer codes can simulate only some aspects of thermomechanical processes in hard rock. Ideally, the code used to model the spent-fuel test in granite should be capable of modeling the following diverse factors:

- Two and three dimensions.
- Heat flow by conduction, convection, and radiation.
- Thermoelasticity.
- Ventilation.
- Excavation.
- Two- and three-dimensional discrete joint models, including dilation.

Many of the codes investigated can handle complex constitutive models of material behavior; however, at this time, no one code is able to model all of the above aspects of the ideal code. Much more code development and verification is necessary to attain the ideal goal.

The spent-fuel test in Climax Stock granite (SFTC) requires calculating the effects of mining and of the storage thermal load on the existing stress fields and the resultant displacement of the rock around the test repository. The thermal loading for each point is affected by heat transfer through conduction, radiation, and normal convection, as well as by ventilation of the storage area. To model the test conditions, we have chosen the ADINA¹ finite-element code to calculate the mechanical effects of mining and thermal loads and the compatible ADINAT² code to model heat flow; these codes presently fulfill several of the requirements listed above for the ideal code.

LAYOUT OF THE TEST REPOSITORY AND ACQUISITION OF DATA

An access shaft was sunk in the Climax Stock granite to the 420-m (1370-ft) level, and three drifts, spaced on 10-m centers, were excavated (Fig. 1). The central drift is used for storage of the spent-fuel canisters and some electrical simulators, and the side drifts contain electrical heaters. A total of 17 vertical storage holes on 3-m centers were sunk in the floor of the central drift to a depth of 6 m (20 ft). Of these holes, 11 are being used for spent-fuel canisters and 6 are being used for electrical simulators. Electrical resistance heaters have been emplaced in vertical holes on 6-m centers in the floors of the side drifts; these heaters will be operated to simulate a large storage array.

Rock temperatures, stresses, and displacements will be measured continually during the anticipated 5-yr storage period, and these measured data will be compared with the calculated results. Instrumentation that has been distributed throughout the test repository includes several hundred thermocouples for measuring temperatures; 26 extensometers with 116 anchor points, along with 34 convergence wire heads with attachment fixtures for tape extensometers, for measuring relative displacements; 21 transducers for monitoring fracture motion; and 18 stress gages. Figure 2 shows an example of one station, where extensometers are installed in both the pillars, in the floor of the central drift, and at two different angles from the side drifts to extend over the central drift. Relative displacements between extensometer heads in the heater drifts and numerous anchor points along the length of the extensometer are being measured.

CALCULATIONAL INPUT

Previously, two-dimensional scoping calculations of the excavation and thermomechanical effects were made with the ADINA and ADINAT codes.³ The inputs to the calculations were based on the conceptual design of the drifts. Temperature-independent values of thermal conductivity and thermal-expansion coefficient and "handbook" values of elastic modulus and Poisson's ratio were used with the thermoelastic model in ADINA. The thermal-decay curve for the spent fuel was based on an estimate of the time of emplacement of the canisters (2.15 yr out of core). In addition, both the radiative heat transfer between the walls

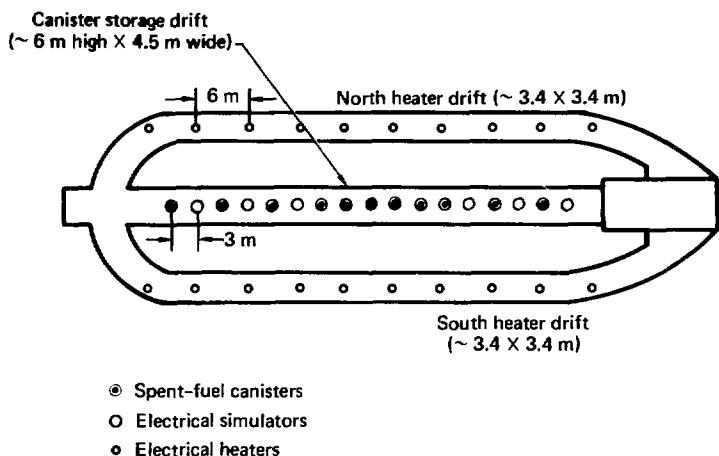


FIG. 1. Layout of the drifts and positions of the spent-fuel canisters, electrical simulators, and electrical heaters.

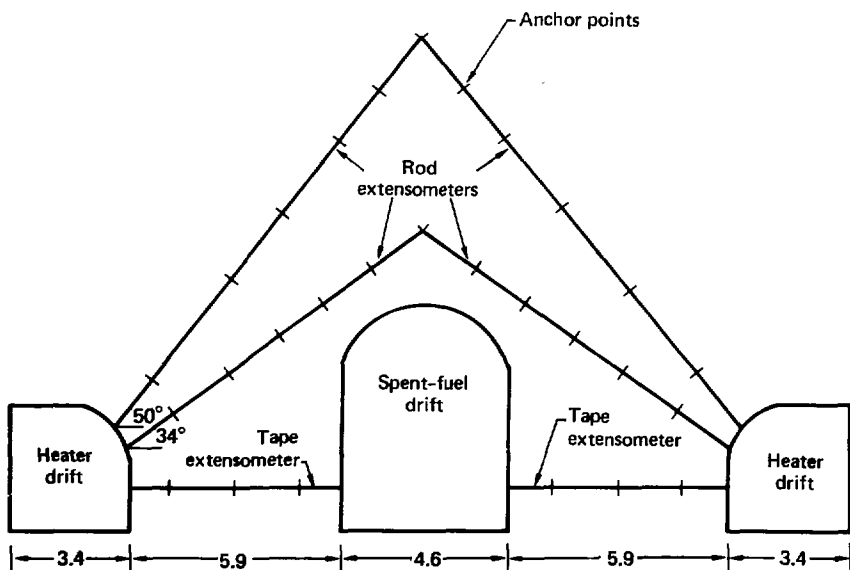


FIG. 2. Layout of one of two extensometer stations, shown in a schematic elevation view through the spent-fuel (central) and heater (side) drifts. The tick marks represent anchor points, to which relative displacements are being measured with respect to hole collars at the walls of the side drifts. Dimensions are in metres.

TABLE 1. Distances used in ADINA and ADINAT calculations.

Cansiter drift	
Floor position	417.58 m below surface 1.75 m above canister top
Cross section	4.98 × 6.25 m domed roof
Heater drift	
Floor position	417.58 m below surface 2.66 m above canister top 3.35 × 3.35 m rounded corner
Spent-fuel canisters and electrical simulators	
Spacing	3 m on center
Length	3.66 m
Electrical resistance heaters	
Spacing	6 m on center
Length	1.83 m

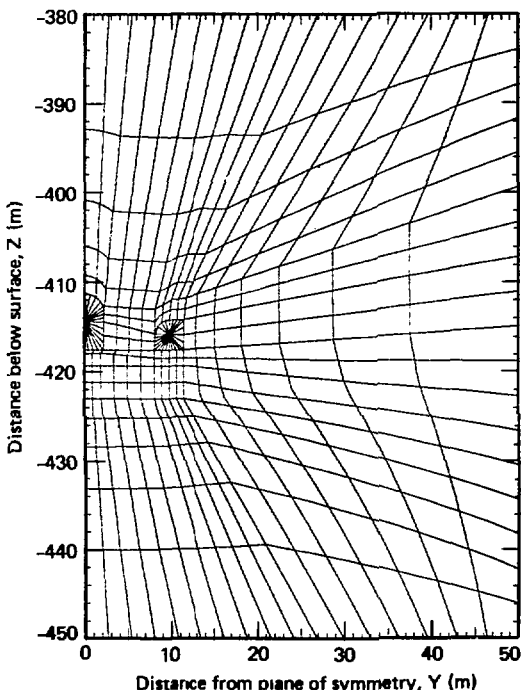


FIG. 3. Finite-element mesh used in the SFTC mining and thermal calculations.

of each drift and the ventilation were rather crudely modeled. Nevertheless, these calculations proved to be extremely valuable in that they provided results that were helpful in selecting positions for instrument placement and for determining the required instrumentation accuracy.

The calculations reported here are also two-dimensional, and the geometry of the drifts is based on "as-built" dimensions. Table 1 shows the distances and spacings used in construction of the finite-element mesh shown in Fig. 3.

Numerical temperature-dependent thermal-expansion coefficients⁴ and temperature-dependent thermal conductivities, based on a suite of measurements,^{5,6} were used in the current calculations. The same investigators^{5,6} do not report temperature-dependent values for heat capacity, elastic modulus, or Poisson's ratio. Values of density, heat capacity, and conductivity of air were used to derive input values for modeling radiative heat transfer and ventilation in the drifts. The power-level decay for the spent fuel was assumed to be proportional to that for PWR fuel with a burnup of 33 000 megawatt days per metric ton of uranium (MWD/MTU) at a specific power of 37.5 MW/MTU.⁷ Table 2 shows material parameters and the heating input to the calculations.

TABLE 2. Material parameters and heating input to the calculations.

Material parameters	
Climax Stock granite	
Density ⁶	2635 kg/m ³
Heat capacity ⁵	930 J/kg-K
Thermal conductivity ^{5,6}	
0°C	3.1679 W/m-K
23°C	3.1184 W/m-K
477°C	2.1184 W/m-K
Thermal expansion ⁴	
0°C	10 × 10 ⁻⁶ K ⁻¹
23°C	10 × 10 ⁻⁶ K ⁻¹
40°C	8.9 × 10 ⁻⁶ K ⁻¹
80°C	7.4 × 10 ⁻⁶ K ⁻¹
125°C	8.0 × 10 ⁻⁶ K ⁻¹
175°C	9.6 × 10 ⁻⁶ K ⁻¹
225°C	12.7 × 10 ⁻⁶ K ⁻¹
Elastic modulus ⁵	48 GPa
Poisson's ratio ⁵	0.21
Air	
Density	1 kg/m ³
Heat capacity	1000 J/kg-K
Thermal conductivity	0.30 W/m-K
Heat parameters	
Spent-fuel canisters and electrical simulators	
Length	3.66 m
Power	1.858 kW (decaying)
Start time = 0	2.45 yr out of core
Electrical resistance heaters	
Length	1.83 m
Power	1.732 kW
Start time	0.3 yr
Ventilation	
Air flow in:	
Spent-fuel drift	1.0 m ³ /s
Heater drifts	0.5 m ³ /s in each drift
Ambient temperature	23°C

THERMAL CALCULATIONS

The thermal calculations were carried out with the ADINAT finite-element code, which is compatible with the ADINA displacement and stress analysis code; i.e., for a given finite-element mesh, ADINAT produces temperature histories for each node in the mesh that is used with the ADINA calculation. Figure 3 shows the mesh used in the calculations. All the elements consist of eight nodes, with the exception of degenerated four-node elements that represent the material in the drifts.

TRUMP,⁸ a multidimensional finite-difference code, correctly models radiative heat transport between the drift surfaces, conductive and convective thermal transport to and through the air in the drifts, and mass flow of the air in the drifts. Unfortunately, a convenient mesh for a TRUMP calculation cannot be used directly with the ADINA code.

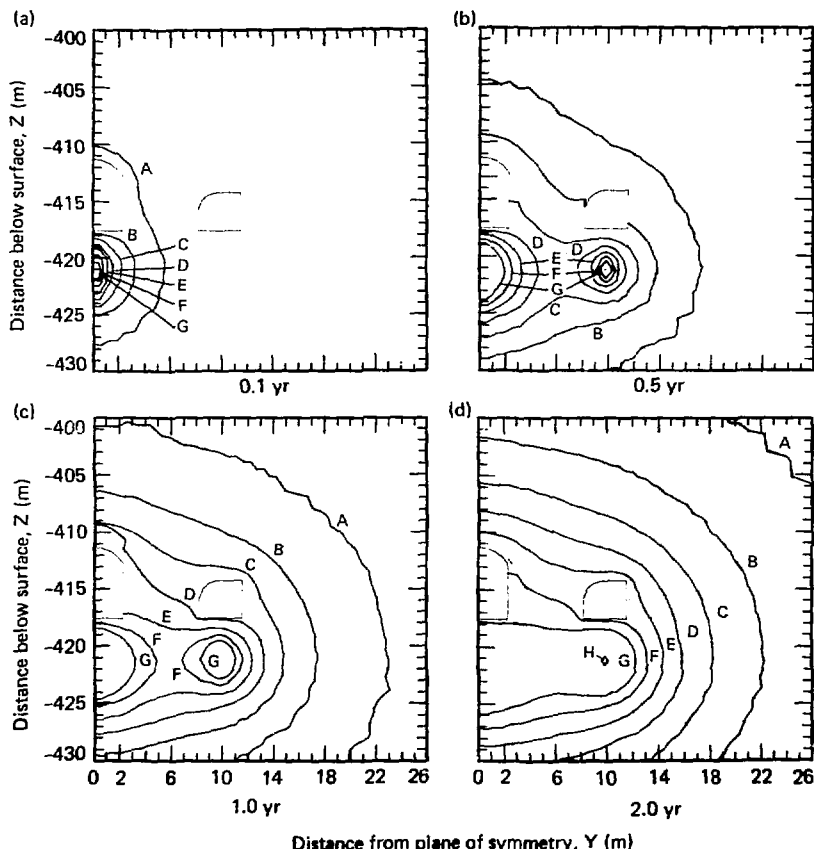


FIG. 4. Temperature contours obtained with ADINAT for various times after emplacement, showing entire mesh. Temperature above ambient, in °C: A = 1, B = 5, C = 10, D = 15, E = 20, F = 25, G = 30, and H = 60.

A method has been devised to enable ADINAT to model internal radiative heat transport and the effects of ventilation.⁹ This method requires that all the side nodes of the drifts be connected with a central node in each drift. Since a TRUMP calculation shows the floor and walls of the drifts to be nearly isothermal, due to radiative heat transfer, radiation flow in the drifts is modeled by assigning to the material in the drifts a high value of thermal conductivity (similar to that of a metal) and a low mass density. Ventilation is modeled by using convective heat transfer from the central nodes to outside the mesh in both drifts. ADINAT calculations were run with input as similar as possible to TRUMP, and the thermal conductivity of the drift material was adjusted until the ADINAT results agreed with the properly modeled TRUMP results.

An ADINAT calculation was run using the material and heat parameters shown in Table 2. Figures 4(a) through 4(d) show contours of the temperatures at different times during the 5-yr test period beginning with an emplacement date of May 1, 1980. The artificially scalloped shapes of the curves result from the method of averaging nodal temperatures in the post processor. Figure 5 shows the maximum extent of the heat flow at 5 yr from startup. The flatness of the curve at the outer boundary of the mesh at $Y = 50$ m is from the boundary condition that fixes the temperature to the ambient.

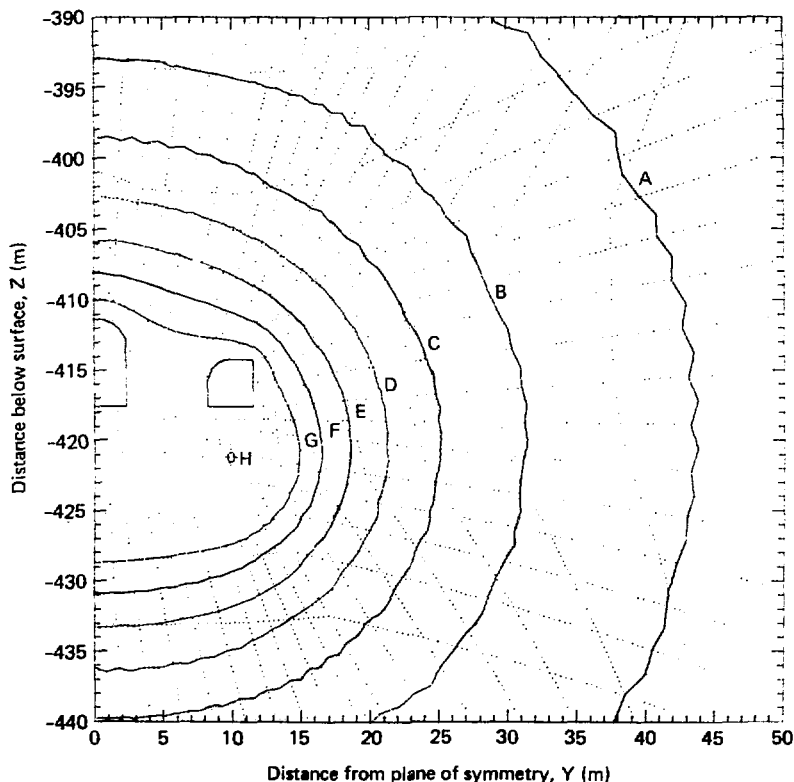


FIG. 5. Temperature contours obtained with ADINAT at 5 yr after emplacement. Temperature above ambient, in °C: A = 1, B = 5, C = 10, D = 15, E = 20, F = 25, G = 30, and H = 70.

THERMOMECHANICAL CALCULATIONS AND RESULTS

An ADINA calculation was run to calculate the effects of both the mining and the later application of the thermal load on the changing stress field and to calculate the resultant displacements. The first four cycles of the calculation related to the application of loads and the mining of the drifts. For this portion of the calculation, Climax Stock granite was assumed to be isotropic linear elastic. Cycle 1 was for the application of the loads. The boundary conditions included using roller boundaries on the axis of symmetry at $Y = 0$, with motion constrained in the Z direction, and at the lower boundary at $Z = -450$ m, constrained from moving in the Y direction (Fig. 3). The upper boundary at $Z = -380$ m and the right boundary at $Y = 50$ m were not constrained; the elements along these boundaries have applied loads, normal to these surfaces, of ρgh , where ρ is the average overburden density, g is the acceleration of gravity, and h is the thickness of the overburden.

Cycles 2, 3, and 4 included the mining portion of the calculations. In cycle 2, the side drifts were excavated by removing all of the elements in the side drifts. In practice, the spent-fuel (central) drift was mined in two passes, the upper, arched, portion first and the lower portion next. Consequently, cycle 3 included excavation of the upper portion, and cycle 4 included excavation of the lower portion. Figures 6(a) through 6(c) show

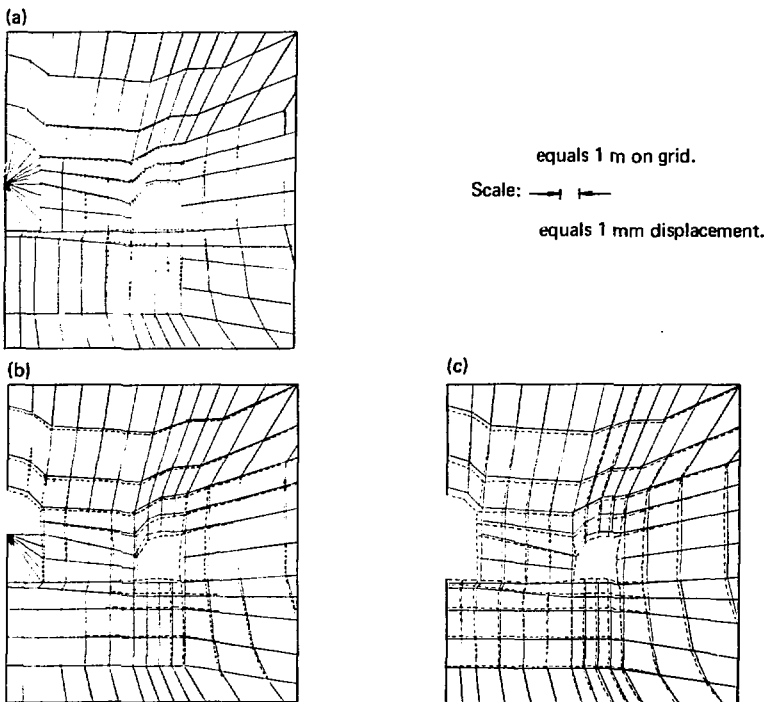


FIG. 6. Displacements due to excavation of the spent-fuel (central) drift and the heater (side) drifts. Maximum displacement is 0.5 mm. (a) Displacement after excavation of heater drift; (b) displacement after excavation of heading of spent-fuel drift; (c) displacement after excavation of bench of spent-fuel drift.

the displacement after each cycle. The displaced shapes have been magnified 1000 times and are shown after each successive portion of the mining. Figures 7(a) through 7(c) show contours of the maximum principal stress after each step of the mining sequence.

The thermal field calculated with ADINAT was imposed during cycles 5 through 204, with cycle time steps of 0.025 yr, or 40 time steps per year for 5 yr. Figures 8(a) through 8(f) show the displacements due to the applied thermal loads at various times during the test. Here, the magnification factor for displacements is 100, rather than the factor of 1000 that was used for the mining portion of the calculation. These thermal displacements include the displacements that arise from mining the central drift. Figures 9(a) through 9(f) show the contours of the maximum principal stress at the same times as those of the thermal displacements. Figures 10(a) through 10(f) show the horizontal (Y-direction) in-plane stress contours, and Figs. 11(a) through 11(f) show the vertical (Z-direction) in-plane stress contours.

SUMMARY AND REMARKS

Thermal and thermomechanical calculations of the spent-fuel test in Climax Stock granite were made before the first spent-fuel canister was emplaced. Inputs to the calculations were based on the "as-built" geometry of the test repository, and measurements of temperature-dependent thermal conductivity, temperature, pressure-dependent thermal-expansion coefficient, and pressure-independent elastic properties were used in the calculations. (Note: elastic properties are, of course, pressure dependent; however, for this calculation, the values for elastic properties were chosen at a pressure equal to that developed by the overburden at the drift depths, so the elastic properties could be considered to be pressure independent.) The calculations also included heat removal by ventilation, and the boundary conditions assumed ρgh preexcavation stress in the rock mass. The results of the calculations are intended to provide a base with which to compare temperature, stress, and displacement data taken during the planned 5-yr duration of the test.

The results of the calculations show the temperature increase above ambient to be of the order of 15°C in the drifts and ribs and 15 to 20°C immediately below the floor of the drifts. The maximum displacements around the drifts from the excavation loads are of the order of a few tenths of millimetres, while the displacements from the applied thermal load are of the order of a few millimetres. The calculated stress fields from both the excavation and the thermal loads are all compressive, ranging from near zero to about 1.76×10^7 Pa (~2500 psi) from the excavation loads and up to about 4.7×10^7 Pa (~6800 psi) from the thermal load.

These calculations are not intended to be predictive. Motion on the existing jointing in the Climax Stock granite can affect the changes in the stress fields and the resultant displacements. The measurement program should provide us with data to determine how the existing jointing influences the results, as compared with an elastic, homogeneous rock mass. If, as expected, the jointing effects are important, new models can be introduced into ADINA to account for these effects.

ACKNOWLEDGMENT

I want to express my appreciation to Russell Greenlaw, of GCN/Hydronet Service, who, as a former employee of LLNL, maintained the ADINAT and ADINA codes and, more recently as a consultant, provided services, particularly with respect to the post processing of the codes' outputs.

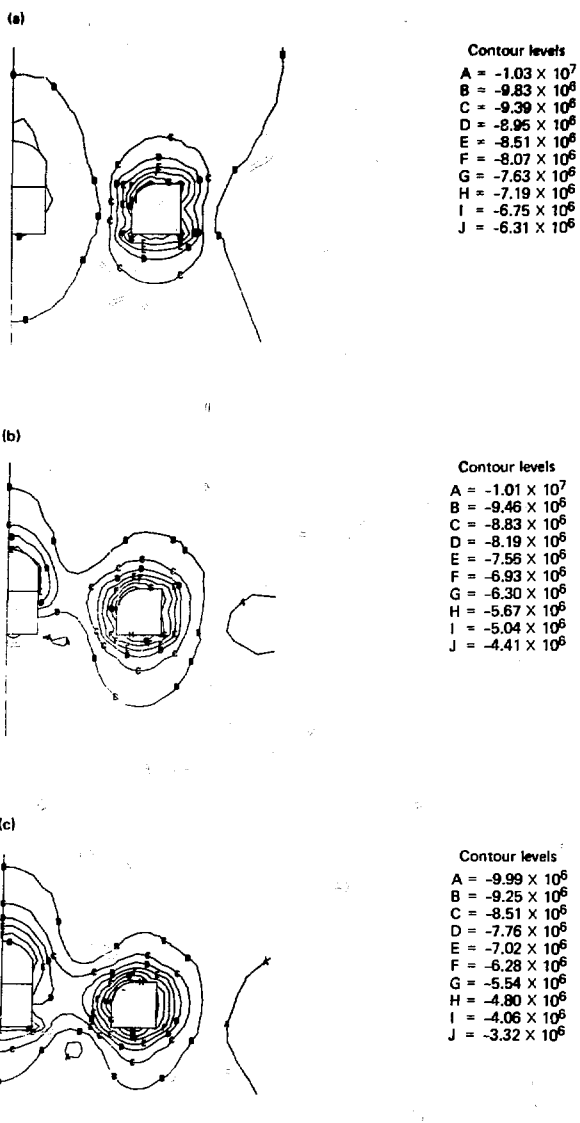


FIG. 7. Contours of maximum principal stress from the effect of mining on the existing imposed stress field: (a) following excavation of header (side) drifts; (b) following excavation of heading of spent-fuel (central) drift; (c) following excavation of branch of spent-fuel drift. Units of stress are pascals (Pa), where $10^5 \text{ Pa} = \text{one bar}$.

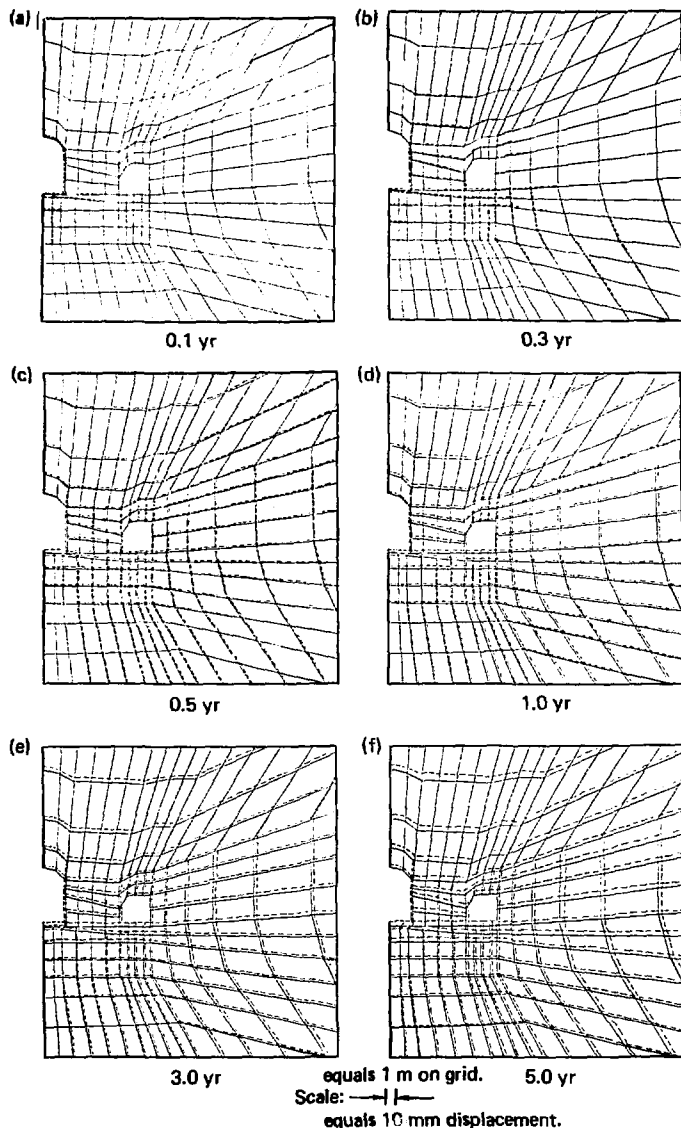


FIG. 8. Displacements due to applied thermal loads from the spent-fuel canisters and the electrical simulators in the spent-fuel (central) drift, from the electrical heaters in the heater (side) drifts, and from ventilation at various times during the test.

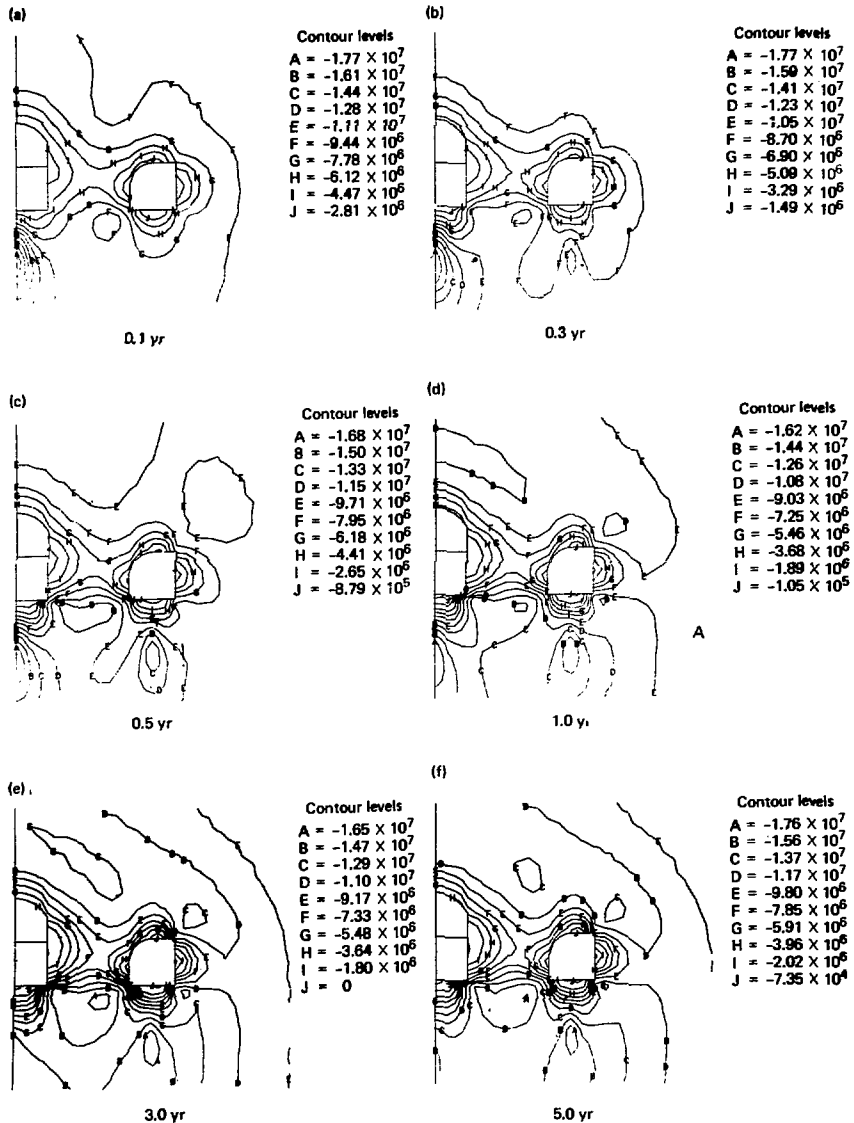


FIG. 9 Contours of maximum principal stress from the effects of the applied heat load on the existing stress field at various times during the test. Units are pascals.

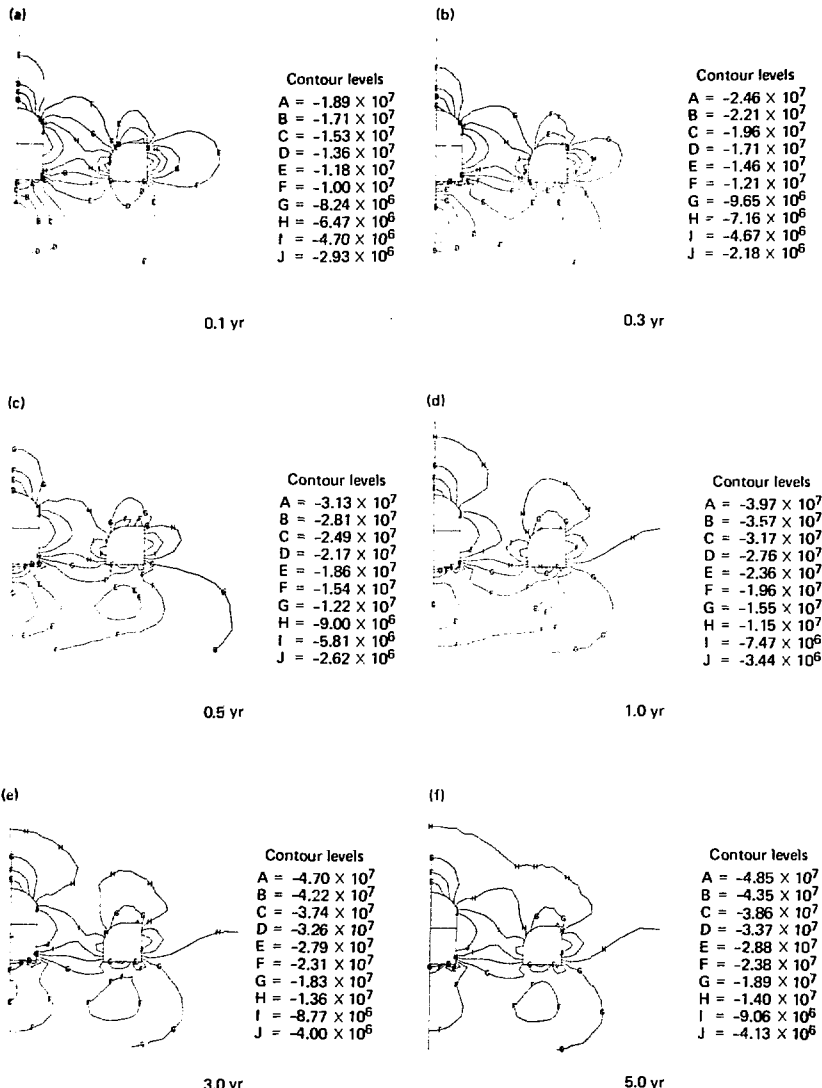


FIG. 10. Contours of horizontal (Y-direction) in-plane stress from the effects of the applied heat load on the existing stress field at various times during the test. Units are pascals.

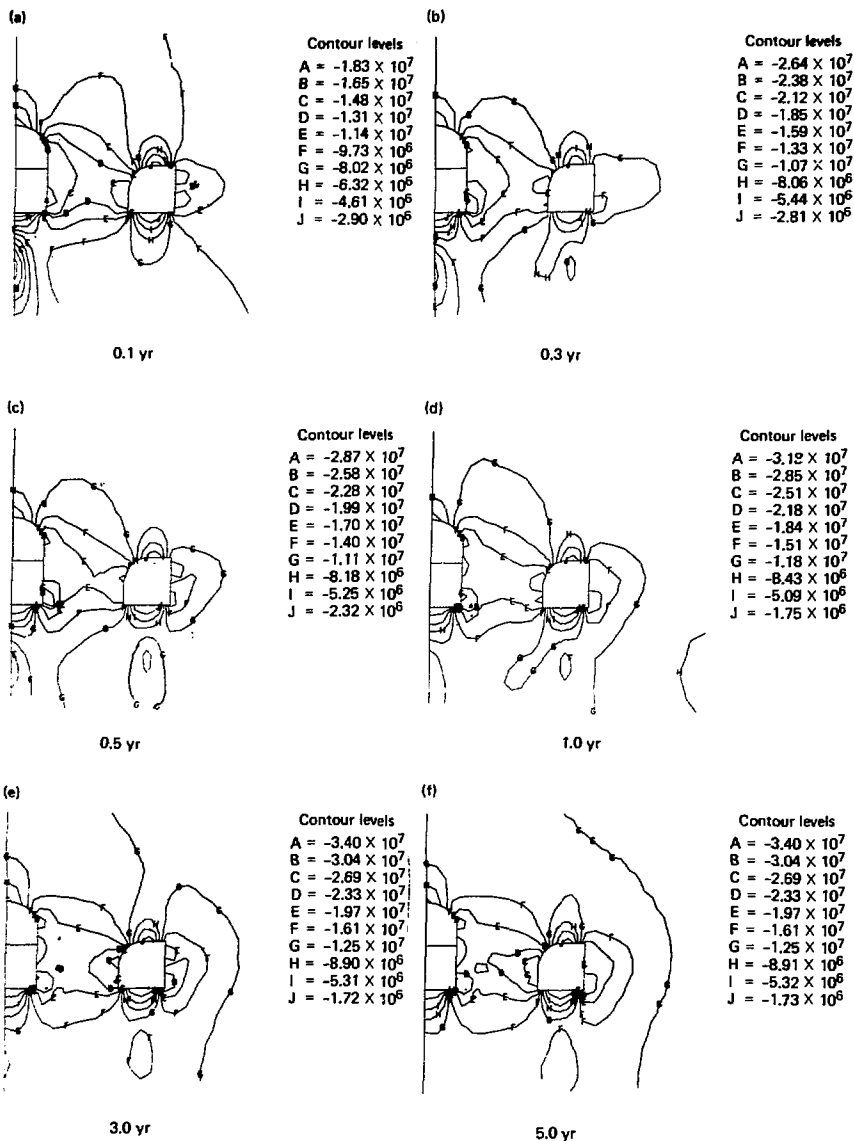


FIG. 11. Contours of vertical (Z-direction) in-plane stress from the effects of the applied heat load on the existing stress field at various times during the test. Units are pascals.

REFERENCES

1. K. J. Bathe, *ADINA. A Finite Element Program for Automatic Dynamic Incremental Nonlinear Analysis*, Massachusetts Institute of Technology, Cambridge, Mass., Report 82448-1 (1978).
2. K. J. Bathe, *ADINAT. A Finite Element Program for Automatic Dynamic Incremental Analysis of Temperature*, Massachusetts Institute of Technology, Cambridge, Mass., Report 82448-5 (1977).
3. R. C. Greenlaw and M. A. Gerhard, *Thermal Analysis of Rock Formation for Nuclear Fuel and Waste Storage*, Lawrence Livermore Laboratory, Livermore, Calif., UCRL-81992 (1979).
4. D. C. Gadd, *Thermal Expansion and Inferred Permeability of Climax Quartz Monzonite to 300°C and 27.6 MPa*, Lawrence Livermore Laboratory, Livermore, Calif., UCRL-83697 (1979).
5. R. Lingle and H. Pratt, *Laboratory Measured Properties of Granodiorite Climax Stock, Nevada Test Site*, Terra Tek Corporation, Report TR-78-47 (1978).
6. H. Pratt, R. Lingle, and T. Schrauf, *Laboratory Measured Material Properties of Quartz Monzonite, Climax Stock, Nevada Test Site*, Lawrence Livermore Laboratory, Livermore, Calif., UCRL-15073 (1979).
7. *Spent Unreprocessed Fuel Facility Engineering Studies*, Rockwell International Corporation, Hanford, Wash., Informal Report RHO-LD-2 (1978).
8. A. L. Edwards, *TRUMP. A Computer Program for Transient and Steady State Temperature Distribution in Multi-dimensional Systems*, Lawrence Livermore Laboratory, Livermore, Calif., UCRL-14754, Rev. 3 (1972).
9. T. R. Butkovich and D. N. Montan, *A Method for Calculating Internal Radiation and Ventilation with the ADINAT Heat-Flow Code*, Lawrence Livermore Laboratory, Livermore, Calif., UCRL-52918 (1980).